LAWRENCE
LIVERMORE
NATIONAL
LABORATORY

LLNL-JRNL-829951

Estimating Explosion Yields using Moment Tensor Solutions and Seismic Moment

M. E. Pasyanos

December 10, 2021

The Seismic Record

Disclaimer

Estimating explosion yields using moment tensor solutions and seismic moment

Michael E. Pasyanos, Lawrence Livermore National Laboratory, Livermore, CA,
pasyanos1@llnl.gov, ORCID 0000-0002-3222-4143

Abstract

Seismic moment, a measurable and well-understood quantity of seismic sources, is used to estimate the yield of explosions. Application of such a method in the past, as in the manner of m_b-derived yields, has been complicated by the effect of variations in the explosion working point, depth, and secondary source effects (such as spalling and tectonic release) on the observed moment. We start by using the full (six-element) moment tensor solution, which can capture the relevant source physics and, at least in theory, better isolate the primary explosion source. The moment-to-yield ratio is then estimated using an explosion source model which, provided with emplacement conditions, can relate the two parameters. We discuss the major sources of uncertainty associated with the method, and calibrate it with chemical and nuclear explosions at the Nevada National Security Site. We then apply the method to published moment tensor solutions for the six declared North Korean nuclear explosions that occurred between 2006 and 2017. The results are mostly consistent with other yield estimates made using a variety of high-frequency methods. This technique is a new approach to estimating explosive yield and simple to implement, as much of the complexity is captured by the source models.

Introduction

Once a seismic event has been positively identified as an explosion, an important step in characterizing the event is to determine the yield. In the past, during active nuclear testing, this was normally accomplished by measuring the teleseismic body wave magnitude m_b and using m_b:yield relationships specifically calibrated for known test sites. These relationships, however, varied significantly from each other based on differing emplacement conditions and earth structure at each test site.

This approach, however, is limited in several ways. First, magnitude is a parameter that was initially developed to relate the relative size of earthquakes to each other, and does not have a physical basis. Because of that, ground truth (GT) knowledge of some of the explosions was necessary to tie the measured magnitudes to yield, and a formula could not be developed if that GT information was absent. Additionally, the relation would not be valid if the conditions (e.g., depth, material properties) were significantly different than the calibration dataset. As a result, the method is not transportable from one test site to another, nor generally applicable to broader regions where explosions might occur. Another issue is that, for smaller events (chemical or nuclear) only recorded at shorter distances, teleseismic m_b may not observed. One workaround for this is to use regional surrogates of m_b, such as m_b(Lg), but these are often subject to large variations in propagation and Lg amplitudes due to tectonic structure. Furthermore, m_b(Lg) is not equivalent to and often significantly biased relative to teleseismic m_b, on which the yield formulas are generally based.

Given the physical nature of seismic moment, moment-derived magnitude M_w (Hanks and Kanamori, 1977) are generally considered to be the magnitude method that best estimates an earthquake size. For many of the same reasons, a moment-based yield estimation method has long been considered a goal for explosion monitoring. One major complicating factor is the presence of secondary source effects, such as tectonic release and free surface interactions, such as spall, which was discussed extensively in Patton (1991). These factors were empirically determined from reduced-order (Isotropic + Double Couple; DC) moment tensors to estimate yield in Ekström and Richards (1994). Patton and Taylor (2011) addressed this by explicitly modeling source medium damage as a compensated linear vector dipole (CLVD) source. Similarly, Howe et al. (2020) expanded from the Ekström and Richards (1994) parameterization, effectively allowing a vertically-oriented CLVD. These previous studies showed that these secondary source effects can bias moment estimates, although none of them calculated full moment tensor solutions, which have the best potential to capture and isolate the non-isotropic components.

In this paper, we expand on some of this previous work to develop a method to estimate physically-based yields for explosions through the use of moment tensor solutions. The approach we take is to tie moment to yield using an explosion source model which relates these two quantities. By using seismic moment and an understanding of how both moment and yield vary as a function of emplacement conditions, the method is or should be transportable to other regions, and applicable to new emplacement conditions. We start by using full (six-component) moment tensor solutions that allows isotropic, DC, and CLVD (including non-vertically-oriented CLVD) components of the explosion source. We will be building on some recent work using

full moment tensor solutions of U.S. underground nuclear tests which confirmed the large effect of material properties on seismic moment generation (Pasyanos and Chiang, 2021).

We first review the background behind an explosion source model and its effect on estimated moment-to-yield ratio under a variety of emplacement conditions. Assuming we know the appropriate moment-to-yield ratio to use, we can then simply calculate an estimated yield directly from the seismic moment. After calibration, we will then apply this methodology to published moment tensor solutions for the six declared North Korean nuclear explosions that were conducted from 2006-2017, and compare the moment-derived yield estimates to other estimates made using different methods. We also discuss the major sources of uncertainty in applying the method before concluding with a discussion of future work.

Background

Our approach in this study is to use an explosion source model to relate seismic moment and explosive yield. We utilize the seismic moment function of Denny and Johnson (1991), in which the moment is proportional to yield. The long-period moment from Denny-Johnson [DJ] was used in the explosion source model of Walter and Ford (2018), a model which was developed in part by noting deficiencies in source models for chemical explosions from the Source Physics Experiments (Ford and Walter, 2013). Although the Walter-Ford [WF] model is a hard-rock model, it is applied to weaker material by modifying the values of Vp, Vs, density, and gas porosity (GP), as appropriate.

Although the models differ from each other in terms of corner frequency, in both the WF and DJ models, the relationship for the seismic moment (Mo) (equation 41 in Denny and Johnson, 1991) is:

$$M_0 = \frac{1}{311} M_t \, {P_0}^{0.3490} \, 10^{-0.0269GP} \quad (1)$$

where M_t is the theoretical moment (= 4/3 π ρ_s α_s^2 R_c^3), P_0 the overburden pressure (=$\rho_s$gz), and GP the gas porosity (in %). Also defined in the paper is the cavity radius R_c (= 1.47x10^4 $W^{(1/3)}$ / $\beta_s^{0.3848}$ $P_0^{0.2625}$ $10^{0.0025GP}$), where W is the yield (in ktons), z the depth (in m), and α_s, β_s, and ρ_s, indicate the material properties (P-wave velocity, S-wave velocity, and density, respectively in MKS units) at the source.

First, expanding all parameters:

$$M_0 = \frac{1}{311}\left[\frac{4}{3}\pi \rho_s \alpha_s^2 \left(1.47 \times 10^4 \, W^{\frac{1}{3}} \beta_s^{-0.3848} (9.81 \, z \, \rho_s)^{-0.2625} \, 10^{-0.0025GP}\right)^3\right]$$
$$(9.81 \, z \, \rho_s)^{0.3490} \, 10^{-0.0269GP} \quad (2)$$

and then combining terms, we are left with:

$$M_0 = 1.57 \times 10^{10} \, W \, \alpha_s^2 \, \beta_s^{-1.1544} \, \rho_s^{0.5615} \, z^{-0.4385} \, 10^{-0.0344 \, GP} \quad (3)$$

Replacing the units of yield from ktons to Joules, the moment-to-yield ratio (Mo/W) in units of N-m/J is:

$$M_0/W = 3.76 \times 10^{-3}\ \alpha_s^2\ \beta_s^{-1.1544}\ \rho_s^{0.5615}\ z^{-0.4385}\ 10^{-0.0344\ GP} \quad (4)$$

While the yield can be estimated by dividing the seismic moment by the right side of equation (4), examining the moment-to-yield ratio provides insight into the effect of emplacement conditions. Whereas the exponents of the material properties (α_s, β_s, ρ_s) vary, the overall effect is for stronger materials to have higher moment-to-yield ratios, and produce larger corresponding seismic signals. Source depth also has an effect on the ratio, with a negative value (-0.4385) in the exponent of depth z indicating that this ratio will decrease with increasing depth (and become infinite at the free surface). Note that, for a given depth, the moment-to-yield ratio is constant, regardless of the yield. This is not the case with explosion source models like Mueller-Murphy (Mueller and Murphy, 1971; MM), in which M_0 is not directly proportional to yield. In practice, models not having moment proportional to yield are more difficult to implement, as the yield would either need to be known (as in the case of testing GT events) or iterated upon.

The change with absolute depth is at least a partial explanation for why chemical explosions, generally at shallower depths, are more efficient generators of seismic energy for a given yield (and observed in the large moment tensor database from Pasyanos and Chiang, 2021). It does not, however, explain the factor of 2 difference observed in the Non-Proliferation Experiment chemical kiloton explosion which was conducted at a depth typical for nuclear explosions

(Denny, 1994). This is usually attributed to the larger momentum provided by chemical explosions, which translates into greater seismic signals for a given yield.

Based on these equations, we compare the expected M_0/W ratio for various materials, starting with granite (**Figure 1a**). Values of Vp, Vs, and density for granite, rhyolite, and tuff (listed in **Table 1**) come from Stevens and Day (1985). The values for alluvium and gas porosity in granite and tuff/rhyolite are derived from Howard (1985), which are used in WF. For tuff and alluvium, we have also created high gas porosity versions of these materials, which we dub "tuff2" and "alluvium2", respectively. The increased values of gas porosity for tuff2 and alluvium2 are derived from the range of values for U.S. underground nuclear explosions (Springer et al., 2002).

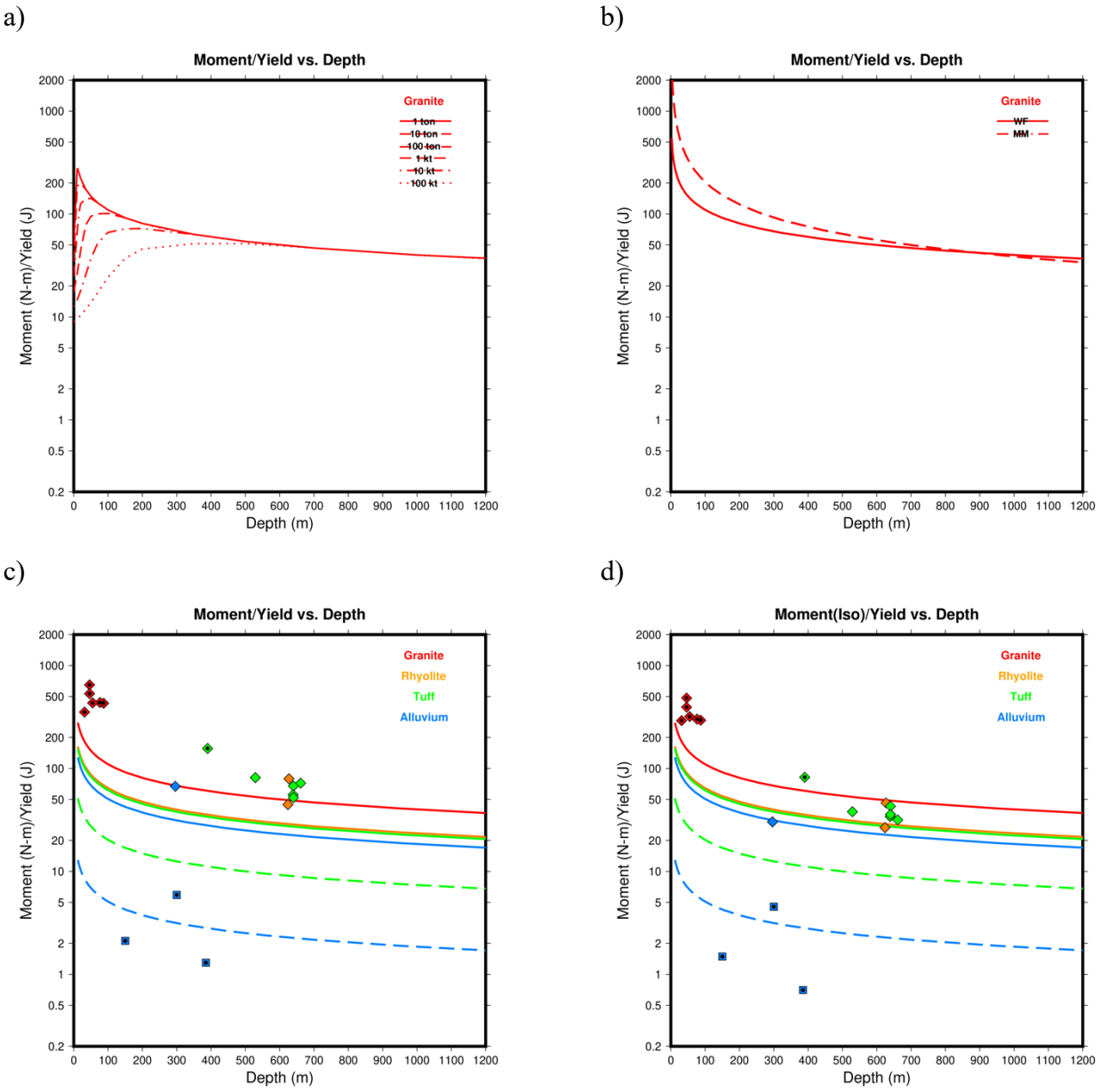

Figure 1. a) Moment-to-yield ratio for granite as a function of depth for different yields showing surface coupling effect. b) A comparison of moment-to-yield ratio as a function of depth between the WF (solid) and MM (dashed) explosion source models. c) A comparison of moment-to-yield ratio as a function of depth for granite (red), rhyolite (orange), tuff (green), tuff2 (dashed green), alluvium (blue), and alluvium2 (dashed blue), along with calculated ratios for nuclear and chemical explosions at the Nevada National Security Site with the moment-to-yield ratio calculated using M_0. Diamonds and squares indicate explosions in regions of low and high GP, respectively. d) The same comparison with the moment-to-yield ratio calculated using isotropic M_0. In both c) and d), points are color-coded by working point material and chemical explosions are indicated with a central black circle.

Table 1. Material parameters

	P-wave velocity (m/s)	S-wave velocity (m/s)	density (kg/m^3)	gas porosity (%)
granite	5500	3175	2550	0.2
rhyolite	3500	2021	2000	1.
tuff	3500	2021	2000	1.
tuff2	3500	2021	2000	15.
alluvium	1600	600	1900	1.
alluvium2	1600	600	1900	30.

P-wave velocity (α_s), S-wave velocity (β_s), density (ρ_s), and gas porosity (GP) for materials shown in **Figure 1**.

Obviously, the seismic moment cannot be infinite, so the moment-to-yield ratio is not infinite at the free surface, as predicted by equation (4). In actuality, as explosions approach the free surface, less energy is coupled into seismic and the moment-to-yield ratio decreases. To demonstrate this, we have taken surface coupling equations (Ford et al., 2014; Pasyanos and Ford, 2015) which model the observed energy loss as a function of scaled depth-of-burial/height-of-burst, which makes the moment-to-yield ratio a function of both yield and depth for near-surface events (**Figure 1a**). For large explosions, the scaled depth is significantly reduced and the explosion starts sensing the surface at greater depths. Events we are using in this study, however, are not significantly underburied, and this is only a minor adjustment.

Figure 1b compares the moment-to-yield ratios for the WF and MM models. For calculation purposes, the yield is set to a scaled depth of 120 m/kt$^{(1/3)}$ (e.g., for 120 m, a 1 kt yield explosion is used). At depths less than 900 m, MM has a higher ratio than WF, significantly so closer to the free surface. The colored line in **Figure 1cd** notes variations due to differences in seismic velocities, say, between hard rock like granite and weaker rock like rhyolite or tuff. While important, however, the deviations are less significant than the extremely large effect of gas porosity on the moment-to-yield ratio. In fact, the difference due to low and high gas porosity on tuff and alluvium is greater than the difference between granite and low GP tuff or alluvium.

Since the accuracy of yield estimates using this method are dependent upon the validity of the explosion source models, we compare predicted ratios from the model with empirical estimates. **Figure 1cd** shows the same moment-to-yield ratio curves along with values for chemical and nuclear explosions at the Nevada National Security Site (NNSS) from Pasyanos and Chiang (2021). As in Chiang et al. (2014), the total scalar moment is calculated using the formulation of Bowers and Hudson (1999). The isotropic component of the moment tensor is calculated as the average of the trace or $(M_{xx}+M_{yy}+M_{zz})/3$. Yields for the nuclear tests shown are taken from the DOE/NV-209. In general, ratios using the total seismic moment (**Figure 1c**) are too high (on average 2.5x as high), and we find a much better fit to the predicted ratios using the isotropic moment (**Figure 1d**). In this case, the ratio between observed and predicted is 1.2 and 1.9 for nuclear and chemical explosions. Notice as well the large difference in ratios for the tests in alluvium. The one nuclear explosion conducted in alluvium is Delphinium, a 15 kt explosion at 970 ft (295 m) (DOE/NV-209) with relatively low GP (5%) which is contrasted with comparable chemical explosions in alluvium which had GPs in excess of 25%. It does appear that, in

general, the chemical explosions are high relative to the nuclear explosions, even considering the depth effect.

Method Testing, Calibration, and Uncertainties

To summarize our approach: First, provided with depth and material properties, the moment-to-yield ratio is calculated using an explosion source model. Next, the seismic moment (potentially either total M_0 or isotropic M_0) is then used to estimate the yield, with an optional correction in the yield for chemical explosions.

We first test and calibrate the method by applying it to events with ground truth (GT) source parameters (yield, depth, working point material). In particular, we are interested in testing the performance of the method against a number of possible variables in the methodology. This includes using total seismic moment M_0 and isotropic moment M_0(Iso), the inclusion of a factor of 2 for chemical explosions, the use of two different explosion source models (WF and MM), and the use of generalized material properties provided in **Table 1** (e.g., "granite") compared to actual measured working point values. Moment values for the explosions come from the full moment tensor database of Pasyanos and Chiang (2021). The GT data for this analysis consists of 18 chemical and nuclear explosions from NNSS with announced yields rather than yield ranges (e.g., 20-150 ktons). Yields and depths of the nuclear explosions are provided in DOE/NV-209, with other values (e.g., working point properties) coming from Springer et al. (2002).

As a baseline, we have taken the regressed M_w:yield relations from Pasyanos and Chiang (2021) and applied them to the test dataset. Misfits in log-yield range from 0.75-0.82 (a factor of ~6 in yield) depending on formulas for M_w or M_w(iso) and those with or without a yield correction for chemical explosions. By applying the new methodology, we improve significantly from this baseline, with **Table 2** summarizing the results. There is a very large difference between using WF and MM models, with the former having much lower misfits. Use of the isotropic moment is better than total moment for the WF model, but not for MM. This makes sense as non-isotropic components of the full moment tensor are primarily due to secondary source effects such as tectonic release and spalling. Again, for WF, modifying the yield of chemical explosions is better than not applying the modification. Surprisingly, using the specific measured material properties is not always an improvement from using the generic specifications of them. This may be due to inadequacies of the explosion source models or to the observed large variability in working point values (Patton and Taylor, 2011). In any case, the best overall results are achieved by using the isotropic moment, the WF explosion source model, generic materials, and by employing a factor of 2 adjustment for chemical explosions. For this combination of parameters, we find a log-yield misfit of 0.301, which corresponds to a factor of 2 in yield.

Table 2. Test of method performance using different variables.

		Walter-Ford		Mueller-Murphy	
		generic mat.	specific mat.	generic mat.	specific mat.
total Mo	$W_C=W_N$	0.438	0.512	0.931	0.870
	$W_C=2 \times W_N$	0.360	0.437	1.07	1.02
isotropic Mo	$W_C=W_N$	0.314	0.375	0.992	0.963
	$W_C=2 \times W_N$	0.301	0.351	1.15	1.12

RMS misfit of estimated yield vs. GT yield for a number of variables (explosion source model, total vs. isotropic moment, material properties, and modification for chemical explosions). The misfit is calculated for base10 log-yield. W_C and W_N refer to chemical and nuclear yields.

We have identified three major sources of uncertainty to this method: 1) depth uncertainties, 2) uncertainties in the explosion source model, and 3) uncertainties in the scalar moment. The first, uncertainties in the estimated depth, can easily be mapped into changes in the moment-to-yield ratio and then into yield. The second source is in the explosion source model, which determines the moment-to-yield based on material conditions and depth. While this source of uncertainty is hard to assess, some insight could be gleaned from a comparison of the variations among various explosion source models including WF/DJ, which use the same moment formula, MM, and others (e.g., Patton, 2012). As demonstrated in MacPhail et al. (2021), there are significant differences among the various models.

The third major source is the uncertainty on the moment tensor or seismic scalar moment itself. While the moment tensor inversion provides formal uncertainties, those resulting from errors in the velocity model are often ignored. Better estimates of true moment tensor uncertainties are

being formulated by way of Bayesian methods that incorporate variations in the velocity model (e.g., Mustać and Tkalčić, 2015). A 1998 Office of Technology Assessment report (OTA, 1988) assessed that M_0 has an uncertainty factor of 2.13, which is consistent with a more recent study by Rösler et al. (2021) that estimated seismic scalar moment uncertainties to be a factor of 2, which translates to 0.2 magnitude units (m.u.) in M_w. In comparison, the OTA report estimated that uncertainties in m_b are 0.3-0.4 m.u. before station corrections and 0.1-0.15 m.u. after station corrections, and yields estimated from m_b and m_b(Lg) have an uncertainty factor of 1.45 and 1.74 at the 95% confidence level.

Application to recent nuclear tests

Moment tensor solutions are taken from the study of Chiang et al. (2018) for the six declared North Korean explosions from 2006-2017, which we have labeled as DPRK1-DPRK6 (**Figure 2** and **Table 3**). Solutions were determined using a time-domain waveform inversion applying the mathematical formulation of Minson and Dreger (2008) to allow for the calculation of the full tensor. Waveform data used in the inversions were from regional stations in China, South Korea, and Japan. Green's functions were calculated using the MDJ2 1D-layered Earth model (e.g., Ford et al., 2009). The period band of analysis was typically 20-50 s, with shorter periods used for DPRK1. The source depth was set to 1000 m for DPRK1 and 600 m for DPRK2-6. As illustrated in **Figure 2**, the estimated moment tensors have a large explosive isotropic component, with percentage isotropic ranging from 72-85%. The remaining components are split between DC (ranging from 1-22%) and CLVD (5-27%). See Table 1 in Chiang et al. (2018) for the specific percentages of ISO, DC, and CLVD for each of the DPRK events.

As a comparison, we have also included in **Table 3** the full moment tensor solutions for the DPRK tests from Alvizuri and Tape (2018) and Alvizuri (2018), which were determined independently. We see an average difference in log-moment of about 0.36 (0.24 m.u. in M_w), which is just larger than a factor of 2 in moment. The difference we see in the isotropic Mo is 0.39 (0.26 m.u.). The largest differences are observed for DPRK2 and DPRK4. Curiously, the Alvizuri moments are larger for the first three explosions, but smaller for the other three.

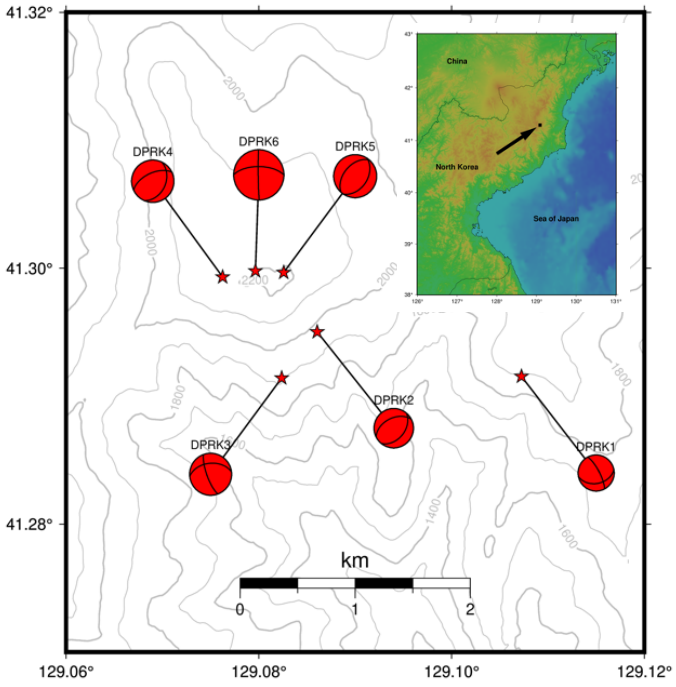

Figure 2. Map showing locations of the six declared DPRK tests, along with their full moment tensor solutions. The inset shows the location of the large-scale map, indicated by the arrow, on a regional topographic map.

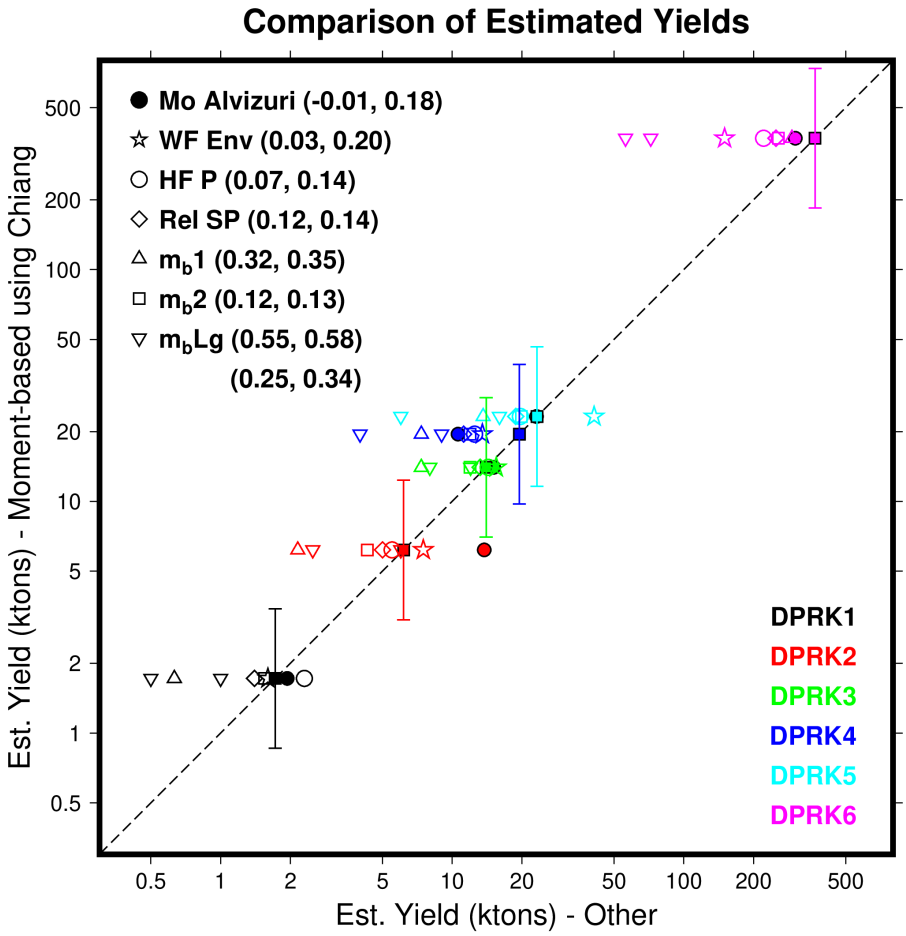

Figure 3. Estimated yields using moment-derived yields using Chiang et al. (2018) moment tensors (filled squares) on the y-axis and comparison yields on the x-axis. Colors indicate the test, while symbols indicate the comparison method: moment-derived yields using Alvizuri and Tape (2018) moment tensors (filled circles), Pasyanos and Myers (2018) waveform envelopes (stars), Voytan et al. (2019) 4 Hz P-waves (circles), and Voytan et al. (2019) relative short period (diamonds), teleseismic m_b using the formula for Semipalatinsk (triangles) and Voytan et al. (2019) (squares), and Xie and Zhao (2018) m_bLg (inverted triangles). Vertical bars are the estimated uncertainties on the moment-based yield estimates. Numbers to the right of the comparison method are mean and rms differences in log-yield.

Based on the results of the previous section, we use the isotropic moment and moment-to-yield ratio from DJ. In calculating the Mo/W, we use material properties for granite, which was

determined by geologic site characterization (Coblentz and Pabian, 2015). As in Pasyanos and Myers (2018), we use as the depth-of-burial the distance from the shot point to the closest surface, rather than the distance to the surface overhead since we feel this better reflects the overburden. This difference is negligible in low relief regions, but can be significant in regions of high relief such as the North Korean test site at Pung'gye Ri. These emplacement conditions are used to determine the moment-to-yield ratio (which varies from 43 to 58) and the moment tensor derived yields, which range from 1.7 - 367 kt (**Table 3**) using the Chiang moment tensor solutions. In comparison, Mo/W varies from 44 to 111 using MM, which would result in smaller estimated yields. Yield estimates uisng the moment tensors of Alvizuri range from 1.9-303 kt, but differ most for DPRK2 and DPRK4 (**Figure 3**).

Uncertainties in the yields are estimated by using a factor of 2 uncertainty in seismic scalar moment and +/- 50 m in overburden. Uncertainties in the material properties are considered to be low given the unlikelihood of high GP in the hard rock of the test site. Uncertainty in the seismic moment dominates and results in a factor of 2 in overall yield uncertainty. Note that moment and yield uncertainties for larger events are larger in an absolute sense, but not in a relative sense. This is because, to first order, uncertainties do not scale with event size, as they are primarily due to the factors previous discussed (e.g. seismic moment, velocity model, depth).

Table 3. Moment estimated yields for the six declared DPRK tests.

Event	Date (yyyy/mm/dd)	Overhead depth (m)	Distance to surface (m)	M_0/W ratio	M_0 (N-m)	M_0(Iso) (N-m)	Estimated Yield (kt)
					Chiang et al. (2018)		
					Alvizuri and Tape (2018)		
DPRK1	2006/10/09	503	424	58.3	5.85e14	4.20e14	1.7 (0.8-3.4)
					7.24e14	4.73e14	1.9 (1.0-3.9)
DPRK2	2009/05/25	621	449	56.8	1.83e15	1.47e15	6.1 (3.1-12.2)
					4.68e15	3.27e15	13.8 (6.9-27.5)
DPRK3	2013/02/12	510	375	61.5	4.86e15	3.61e15	14.0 (7.0-28.0)
					5.96e15	3.89e15	15.1 (7.6-30.2)
DPRK4	2016/01/06	772	594	50.3	4.82e15	4.10e15	19.4 (9.7-38.8)
					2.99e15	2.23e15	10.6 (5.3-21.2)
DPRK5	2016/09/09	772	578	50.4	6.84e15	4.95e15	23.1 (11.0-46.2)
					6.61e15	4.93e15	23.1 (11.6-46.2)
DPRK6	2017/09/03	776	637	43.6	8.06e16	6.73e16	367.4 (183.7-734.8)
					7.41e16	5.53e16	303.0 (151.5-605.9)

Scalar seismic moment M_0 and isotropic moment M_0(Iso) for the six tests from Chiang et al. (2018) (top row in right three columns) and Alvizuri and Tape (2018) (bottom row in right three columns). Depths to both overhead surface and to closest surface from Pasyanos and Myers (2018) are provided. The moment-to-yield ratio provided is for the DJ/WF model. Estimated yields in the last column is accompanied by uncertainty range.

In addition to the comparison between moment-derived yield estimates, we compare yield estimates for the DPRK tests to several other estimates: 1) regional waveform envelopes (Pasyanos and Myers, 2018), 2) high-frequency P-waves (Voytan et al., 2019), 3) relative short-period waveform equalization (Voytan et al., 2019), 4) teleseismic m_b using the formula of Ringdal et al. (1992), 5) teleseismic m_b using the formula of Voytan et al. (2019), and 6) regional

m_bLg (Xie and Zhao. 2018). For the last study, m_bLg yields are plotted for both scaled depth (smaller yield) and adjusted depth (larger yield). One advantage of moment-derived yield relative to others is that there is a more direct estimation of long-period signal using moment tensors (20-50 sec) and less extrapolation than higher frequency methods (generally >0.5 Hz) which are more susceptible to propagation variations and make assumptions about spectral shape and corner frequency. **Figure 3** shows the comparison, along with mean and rms differences, which shows that, in general, this method is more consistent with the first three methods than with m_b-derived yields. The one exception is for yields determined using one specifically determined for the North Korean test site (m_b2), rather than regressions adapted from other regions (m_b1, m_bLg).

Conclusions, Discussion, and Future Work

We have presented a new method of estimating the yield of explosions using moment tensor solutions and seismic moment. We calibrate the method against a select data set of explosions conducted at NNSS with announced yields before applying the technique to declared DPRK nuclear explosions. The use of the isotropic moment appears to minimize secondary source effects, which can bias yield estimates. The DPRK yield estimates are generally consistent with other estimates, although generally higher than m_b-derived yield estimates. Other long-period yield estimates, such as M_S-derived yield (e.g., Bonner et al., 2008) can be significantly affected by secondary source effects but, unlike with moment tensors, they cannot be easily removed. We have discussed the major sources of uncertainties, which need to be better understood and characterized if the method is to be used reliably on a regular basis. In general, the largest source

of uncertainty is in the seismic scalar moment itself, although this could be reduced through the use of 3-D velocity models in the moment tensor Green's functions (e.g., Nayak and Dreger, 2018) and better depth resolution. And, while uncertainties are comparable to those from other calibrated methods, this approach has the advantage of being transportable to other regions without calibration.

The methodology described in this paper provides an innovative approach to yield estimation. The method is easy to understand and straightforward to apply. It uses estimates of the seismic moment from full moment tensor solutions along with source models which can relate the observed moment to yield, according to the specific emplacement conditions. Implementation is simple because the complexities of the emplacement conditions are captured by the explosion source model. This study is a demonstration of the method. A more comprehensive analysis of the method will be made on the complete moment tensor database.

The method is applicable to a large class of events. Our tests have applied the method to events spanning over six orders of magnitude in yield, from sub-ton chemical explosions to nuclear explosions greater than 100 ktons. Because it can readily accommodate differences in emplacement conditions, it is a universal method that is transportable from region to region, as demonstrated by its application to explosions in the western U.S. and east Asia. As a physics-based technique, it is also potentially applicable to low yield explosions. The approach taken here used waveform modeling to estimate the full moment tensor solution, in order to remove secondary source effects and best isolate the primary explosion source. If, however, the non-isotropic components of the moment tensor (DC, CLVD) are either assumed or determined to be

small, coda-derived moments (e.g. Mayeda et al., 2003) could be used to extend this analysis to even lower yield explosions. Chiang et al. (2018) found that the coda magnitude estimates for the six DPRK events deviated less than 0.1 m.u. from the moment tensor derived magnitudes.

In the future, we would like to apply the method to a large assortment of chemical and nuclear explosions occuring in different geographic regions and in a diversity of materials. GT yields for nuclear explosions, however, are often difficult to come by. Yields for events in many earlier studies on moment-derived yields were actually m_b-derived yields. In addition to fully exploring the relative magnitude of the uncertainties identified in this study, we would also like to the apply the method to near surface events where the explosions are not as fully coupled seismically as deeper events.

Data and Resources

All data used in this paper came from published sources listed in the references.

Declaration of Competing Interests

The author declares no competing interests.

Acknowledgments - We thank Andrea Chiang, Sean Ford, Gene Ichinose, and Bill Walter for their review of the work. This work was performed under the auspices of the U.S. Department of Energy by Lawrence Livermore National Laboratory under Contract DE-AC52-07NA27344, and is document LLNL-JRNL-829951. This work was supported by the Office of Defense Nuclear

Nonproliferation Research and Development within the U.S. Department of Energy's National Nuclear Security Administration.

References

Alvizuri, C., and C. Tape (2018). Full moment tensor analysis of nuclear explosions in North Korea, Seism. Res. Lett., 89, 2139–2151, doi: 10.1785/0220180158.

Alvizuri C. (2018). Seismic moment tensor results for nine events in the North Korea region, ScholarWorks@UA, descriptor file with figures, text files of catalog, and input weight files, available at http://hdl.handle.net/11122/8441.

Bonner, J., R.B. Herrmann, D. Harkrider, and M. Pasyanos (2008). The surface wave magnitude for the 9 October 2006 North Korean nuclear explosion, Bull. Seism. Soc. Amer. 98, 2498–2506. doi:10.1785/0120080929.

Bowers, D. and J.A. Hudson (1999). Defining the scalar moment of a seismic source with a general moment tensor, Bull. Seism. Soc. Amer., 89, 1390-1394, doi: 10.1785/BSSA0890051390.

Chiang, A., D.S. Dreger, S.R. Ford, and W.R. Walter (2014). Source characterization of underground explosions from combined regional moment tensor and first-motion analysis. Bull. Seism. Soc. Amer., 104, 1587–1600, doi: 10.1785/0120130228

Chiang, A., G.A. Ichinose, D.S. Dreger, S.R. Ford, E.M. Matzel, S.C. Myers, and W.R. Walter (2018). Moment tensor source-type analysis for the Democratic People's Republic of Korea–declared nuclear explosions (2006–2017) and 3 September 2017 collapse event. Seism. Res. Lett., 89, 2152–2165, doi:10.1785/0220180130.

Coblentz, D. and F. Pabian (2015). Revised geologic site characterization of the North Korean test site at Punggye-ri, Science & Global Security, 23, 101-120, doi: 10.1080/08929882.2015.1039343.

Denny, M.D. and L.R. Johnson (1991). The explosion seismic source function: models and scaling laws reviewed, in Explosion Source Phenomenology, Am. Geophys. Monograph, 65, 1–24, doi:10.1029/GM065p0001.

Denny, M.D. (1994). Introduction and highlights, in Proceedings of the Symposium of the Non-Proliferation Experiment (NPE): Results and Implications for Test Ban Treaties, Rockville, MD, 19–21 April 1994, 1–1 – 1-13.

Ekström, G. and P.G. Richards (1994). Empirical measurements of tectonic moment release in nuclear explosions from teleseismic surface waves and body waves, Geophys. J. Int., 177, 120-140, doi:10.1111/j.1365-246X.1994.tb03307.x

Ford, S.R., D.S. Dreger, and W.R. Walter (2009). Source analysis of the Memorial Day explosion, Kimchaek, North Korea, Geophys. Res. Lett., 36**,** L21304, doi:10.1029/2009gl040003.

Ford, S. and W.R. Walter (2013). An explosion model comparison with insights from the Source Physics Experiments, Bull. Seism. Soc. Amer., 103, 2937-2945, doi:10.1785/0120130035.

Ford, S., A.J. Rodgers, H. Xu, D.C. Templeton, P. Harben, W. Foxall, and R.E. Reinke (2014). Partitioning of seismoacoustic energy and estimation of yield and height-of-burst/depth-of-burial for near-surface explosions, Bull. Seism. Soc. Amer., 104, 608-623, doi:10.1785/0120130130.

Hanks, T.C. and H. Kanamori (1979). A moment magnitude scale, J. Geophys. Res., 84, 2348-2350, doi:10.1029/JB084iB05p02348.

Howard, N.W. (1985). Variation in properties of nuclear test areas and media at the Nevada Test Site, UCRL-53721, Lawrence Livermore National Laboratory, Livermore, California, 48 pp.

Howe, M., G. Ekström, and P.G. Richards (2020). Vertical force scaling in seismic source models of underground nuclear explosions, Geophys. J. Int., 221, 251-264, doi:10.1093/gji/ggz582.

MacPhail, M.D., B.W. Stump, and R.-M. Zhou (2021). The effects of assumed source depth and shear-wave velocity on moment tensors estimated for small, contained chemical explosions in granite. Bull. Seism. Soc. Amer., 111, 541–557. doi:10.1785/0120200163.

Mayeda, K., A. Hofstetter, J.L. O'Boyle, and W.R. Walter (2003). Stable and transportable regional magnitudes based on coda-derived moment-rate spectra, Bull. Seismo. Soc. Amer., 93, 224–239, doi:10.1785/0120020020.

Minson, S.E. and D.S. Dreger (2008). Stable inversions for complete moment tensors. Geophys. J. Int., 174(2), 585–592. doi:10.1111/j.1365-246X.2008.03797.x.

Mueller, R.A. and J.R. Murphy (1971). Seismic characteristics of underground nuclear detonations, I: seismic spectrum scaling, Bull. Seism. Soc. Amer., 61, 1675-1692, doi:10.1785/BSSA0610061675.

Mustać, M. and H. Tkalčić (2016). Point source moment tensor inversion through a Bayesian hierarchical model, Geophys. J. Int., 204, 311–323, doi:10.1093/gji/ggv458.

Nayak, A., and D.S. Dreger (2018). Source inversion of seismic events associated with the sinkhole at Napoleonville salt dome, Louisiana using a 3-D velocity model, Geophys. J. Int., 214, 1808–1829, doi: 10.1093/gji/ggy202.

Pasyanos, M.E. and S.R. Ford (2015). Determining the source characteristics of explosions near the Earth's surface, Geophys. Res. Lett., 42, 3786-3792, doi:10.1002/2015GL063624.

Pasyanos, M.E. and S.C. Myers (2018). The coupled location/depth/yield problem for North Korea's declared nuclear tests, Seism. Res. Lett., 89, 2059-2067, doi:10.1785/0220180109.

Pasyanos, M.E. and A. Chiang (2021). Full moment tensor solutions of U.S. underground nuclear tests for event screening and yield estimation, Bull. Seism. Soc. Amer., 112, 538–552, doi:10.1785/0120210167.

Patton, H.J. (1991). Seismic moment estimation and the scaling of the long-period explosion source spectrum. In Explosion Source Phenomenology (eds S.R. Taylor, H.J. Patton and P.G. Richards), doi:10.1029/GM065p0171.

Patton, H.J. and S.R. Taylor (2011). The apparent explosion moment: Inferences of volumetric moment due to source medium damage by underground nuclear explosions. J. Geophys. Res., 116, doi:10.1029/2010JB007937.

Patton, H. J. (2012). A revised cavity radius scaling relationship for explosions detonated in a granite medium, Los Alamos National Laboratory, LA-UR-12-27099, pp. 12.

Ringdal, F., P.D. Marshall, and R.W. Alewine (1992). Seismic yield determination of Soviet underground nuclear explosions at the Shagan River test site, Geophys. J. Int. 109, 65–77, doi:10.1111/j.1365-246X.1992.tb00079.x.

Rösler, B., S. Stein, and B.D. Spencer (2021). Uncertainties in seismic moment tensors inferred from differences between global catalogs. Seism. Res. Lett., 92, 3698-3711, doi:10.1785/0220210066.

Springer, D.L., G.A. Pawloski, J.L. Ricca, R.F. Rohrer, and D.K. Smith (2002). Seismic source summary for all U.S. below-surface nuclear explosions, Bull. Seism. Soc. Amer., 92, 1806-1840, doi: 10.1785/0120010194.

Stevens, J. and S.M. Day (1985). The physical basis of mb:Ms and variable frequency magnitude methods for earthquake/explosion discrimination, J. Geophys. Res., 90, 3009-3020, doi:10.1029/JB090iB04p03009.

U.S. Congress Office of Technology Assessment (1988). "Seismic Verification of Nuclear Testing Treaties", OTA-ISC-361, U.S. Government Printing Office, Washington, D.C.

U.S. Department of Energy, Nevada Operations Office (2015). United States Nuclear Tests: July 1945 through September 1992, Department of Energy, DOE/NV-209, Rev. 16, September 2015.

Voytan, D., T. Lay, E. Chaves, and J. Ohman (2019). Yield estimates for the six North Korean nuclear tests from teleseismic P wave modeling and intercorrelation of P and Pn recordings. J. Geophys. Res., 124, 10.1029/2019JB017418.

Walter, W.R. and S.R. Ford (2018). A preliminary explosion seismic spectral model for saturated/hard rock, Tech. Rept. LLNL-TR-754292, Lawrence Livermore National Laboratory, Livermore, CA.

Xie, X.-B, and L.-F. Zhao (2018). The seismic characterization of North Korea underground nuclear tests. Chinese Journal of Geophysics, 61(3): 889-904. doi: 10.6038/cjg2018L0677.

List of Figure Captions

Figure 1. a) Moment-to-yield ratio for granite as a function of depth for different yields showing surface coupling effect. b) A comparison of moment-to-yield ratio as a function of depth between the WF (solid) and MM (dashed) explosion source models. c) A comparison of moment-to-yield ratio as a function of depth for granite (red), rhyolite (orange), tuff (green), tuff2 (dashed green), alluvium (blue), and alluvium2 (dashed blue), along with calculated ratios for nuclear and chemical explosions at the Nevada National Security Site with the moment-to-yield ratio calculated using M_0. Diamonds and squares indicate explosions in regions of low and high GP, respectively. d) The same comparison with the moment-to-yield ratio calculated using isotropic M_0. In both c) and d), points are color-coded by working point material and chemical explosions are indicated with a central black circle.

Figure 2. Map showing locations of the six declared DPRK tests, along with their full moment tensor solutions. The inset shows the location of the large-scale map, indicated by the arrow, on a regional topographic map.

Figure 3. Estimated yields using moment-derived yields using Chiang et al. (2018) moment tensors (filled squares) on the y-axis and comparison yields on the x-axis. Colors indicate the test, while symbols indicate the comparison method: moment-derived yields using Alvizuri and Tape (2018) moment tensors (filled circles), Pasyanos and Myers (2018) waveform envelopes (stars), Voytan et al. (2019) 4 Hz P-waves (circles), and Voytan et al. (2019) relative short period (diamonds), teleseismic mb using the formula for Semipalatinsk (triangles) and Voytan et al. (2019) (squares), and Xie and Zhao (2018) mbLg (inverted triangles). Vertical bars are the estimated uncertainties on the moment-based yield estimates. Numbers to the right of the comparison method are mean and rms differences in log-yield.

mailing address:
Michael E. Pasyanos, Lawrence Livermore National Laboratory, L-046, P.O. Box 808, Livermore, CA, 94551